## Least-squares wave-equation AVP imaging of 3D common azimuth data

*Juefu Wang *Henning Kuehl, and Mauricio D. Sacchi*

### Summary

This paper summarizes our experience with 2D/3D least-squares amplitude versus Angle (AVA) migration. AVA imaging can be posed as a linear inverse problem. This provides several advantages. First, we are able to incorporate model space weighting operators that improve amplitude fidelity in common angle gathers. In addition, the influence of improperly sampled data can be diminished. The latter leads to the attenuation of acquisition footprints.

In order to make our problem computationally tractable, we utilize 3D common azimuth wavefield modeling and migration operators (Biondi and Palacharla, 1996). The inversion algorithm uses the method of conjugate gradients. We show that robust estimates of AVA attributes can be obtained by properly selecting the model and data space regularization operators. Finally, it is important to stress that the inversion of AVA gathers is the first step toward a robust and accurate estimation of physical rock properties and fluid indicators from surface seismic records.

Our numerical implementation of LS wave equation AVA imaging is tested with a 3-D common azimuth data set from the Western Canadian Sedimentary Basin.

### Introduction

Common image gathers in angle domain (Stolt and Weglein, 1985; de Bruin et al., 1990) contain valuable angle dependent amplitude information. For this reason, AVA/AVP migration has gained increasing interest in recent years (Xu et al., 1998; Prucha et al., 1999; Wapenaar et al., 1999; Mosher and Foster, 2000; Sava et al., 2001). Kuehl and Sacchi (2001, 2002) showed that regularized least-squares wave equation migration could be used to mitigate imaging artifacts and acquisition-induced artifacts caused by missing observations.

In this article, we present an extension of the 2D AVA inversion algorithm proposed by Kuehl and Sacchi (2001) to the 3D case. We use the common azimuth operator proposed by Biondi and Palacharla (1996) in conjunction with a combination of a PSPI (phase shift plus interpolation) and split step correction in order to account for lateral velocity variations in the 3D macro velocity field in both the forward (de-migration) and adjoint (migration) operators that are required by the inversion scheme. Common azimuth migration permits us for a considerable reduction of the data size and computational cost of 3D migration. This is crucial for any attempt to implement least-squares migration on 3D field data.

### 3-D common azimuth AVA imaging

Biondi and Palacharla (1996) proposed a phase-shift migration operator for 3-D common azimuth data. The algorithm downward continues the surface wavefield using the following propagation scheme:

$$\begin{aligned} P(z+dz,\omega,k_{mx},k_{my},k_{hx}) = \\ P(z,\omega,k_{mx},k_{my},k_{hx}) \cdot e^{-ik_z dz} \end{aligned} \quad (1)$$

Where the vertical wavenumber is calculated by a modified double square root equation:

$$\begin{aligned} k_z = \omega\Big(\sqrt{\tfrac{1}{v(r,z)^2} - \tfrac{1}{4\omega^2}[(k_{mx}+k_{hx})^2 + (k_{my}+\hat{k}_{hy})^2]} \\ + \sqrt{\tfrac{1}{v(s,z)^2} - \tfrac{1}{4\omega^2}[(k_{mx}-k_{hx})^2 + (k_{my}-\hat{k}_{hy})^2]}\Big) \end{aligned} \quad (2)$$

$v(r,z)$ and $v(s,z)$ are the velocities evaluated at depth $z$ and source and receiver lateral locations $r$ and $s$. These velocities are replaced with the average velocity $v_m(z)$ at a given depth $z$ . Lateral velocity variation effects can be alleviated with velocity-correction terms like the prestack split-step correction (Popovici, 1996). For large velocity variations PSPI (Gazdag and Sguazzero, 1984) in conjunction with split-step is adopted (Kuehl and Sacchi, 2003). The spatial frequencies $k_{mx}$ and $k_{my}$ are the midpoint wavenumbers in in-line and cross-line directions, respectively. In addition, $k_{hx}$ is in-line offset wavenumber. The resulting expression for $\hat{k}_{hy}$ is obtained by using the stationary phase approximation (Biondi and Palacharla, 1996):

$$\hat{k}_{hy}(z) = k_{my} \times \frac{\sqrt{\frac{1}{v_m^2} - \frac{1}{4\omega^2}(k_{mx}+k_{hx})^2} - \sqrt{\frac{1}{v_m^2} - \frac{1}{4\omega^2}(k_{mx}-k_{hx})^2}}{\sqrt{\frac{1}{v_m^2} - \frac{1}{4\omega^2}(k_{mx}+k_{hx})^2} + \sqrt{\frac{1}{v_m^2} - \frac{1}{4\omega^2}(k_{mx}-k_{hz})^2}} \quad (3)$$

Equations (2) and (3) provide a routine to back propagate energy to different depths. At each depth, we can image the wavefield at zero time by considering the following two steps. First, we use the radial-trace transform (Sava et al, 2001) to compute the contribution to the image of waves propagating with ray parameter $p_{hx}$ . The relationship between offset ray parameter $p_{hx}$ , frequency $\omega$ and offset wavenumber $k_{hx}$ is straightforward:

$$p_{hx} = \frac{k_{hx}}{\omega} \quad (4)$$

The second step is to sum all traces along radial lines in $(k_{hx}, \omega)$ domain with slope $p_{hx}$ (Mosher and Foster, 2000). The above algorithm produces Common Image Gathers (CIG) in the ray parameter domain. These image gathers can be transformed to angle domain by the following expression:

$$sin\theta = \frac{v(m,z)p_{hx}}{2cos\phi} \quad (5)$$

where $\theta$ is the incident angle, $v(m,z)$ is the velocity at the midpoint position $m$ and $\phi$ is the dip angle of the interface.

## Least-squares wave equation AVA Imaging

We consider seismic data as the result of a linear transformation on an earth model $m$

$$d = Lm + n \quad (6)$$

where $d$ denotes the observed data, $L$ is the forward operator, $m$ is common image gather, and $n$ is the noise. Conventional migration entails applying $L'$ , the adjoint of $L$, to the observed data. The anatomy of the operators $L$ and $L'$ is described in detail in Kuehl and Sacchi (2003). In our algorithm, $m$ represent the reflection strengh at midpoint location $x, y$ and depth $z$ versus ray parameter $p_{hx}$, whereas $d$ represents common azimuth 3D data.

When the data are properly sampled, the amplitude in the CIG can be corrected by incorporating the Jacobian correction Sava (2001). This correction attempts to make the adjoint operator behave like the inverse operator. In general, this correction might not be sufficient to achieve good amplitude fidelity. Sampling and migration artifacts are not suppressed by this correction. These artifacts can be attenuated, however, by constraining the solution to exhibit certain degree of smoothness along the ray parameter axis. In this case, we adopt the following cost function to retrieve a migrated image that "fits" the observations and, in addition, exhibits smoothness or continuity along the ray parameter axis:

$$F(m) = ||W(d - Lm)||^2 + \lambda^2 ||D_{1hx} m||^2 \quad (7)$$

where $W$ is a diagonal weighting matrix used to decrease the influence of "bad data" (missing observations) in the migrated image. The operator $D_{1hx}$ is a first order derivative operator along the in-line ray parameter-offset direction. Least-squares migration seeks a model $m$ by minimizing the sum of the two norms. The trade-off parameter $\lambda$ determines the amount of smoothing. We minimize the objective function using a conjugate gradients algorithm (Hestenes and Stiefel, 1952). In this case, the algorithm reduces to the sequential application of the following operators: migration ($L'$), de-migration ($L$), smoothing ($D_{1hx}$) and, sampling ($W$). It is important to stress that these operators are applied in the flight; in other words, there is no need of constructing equivalent operators in matrix form.

## Field data example

We tested our least-squares common azimuth migration algorithm using the Erskine data set provided by Veritas Geo-services. The data were first binned, and ensembles of common azimuth were created. The binned data consist of 157 in-lines and 40 cross-lines. The offset dimension ranges from zero to 3000 meters. The distribution of offset is highly uneven (Figure 1). Rather than attempting to interpolate the data before migration, we have utilized the least squares migration algorithm outlined in the previous section. In particular, we have used the diagonal matrix of weights $W$ to undertone the influence of missing offset position in each cdp bin.

Figure 2 (A) portrays the AVP gather obtained for midpoint CMP position crossline#36, inline#71 (Figure 1) in the inline direction. This AVP image corresponds to the migration of the binned data without any attempt to interpolation (zeros traces were assigned to missing offset positions). Artifacts along ray parameter, an effect caused by irregular/incomplete data sampling, are clearly seen. Figures 2 (B) portrays the least-squares inverted CIG after 4 iterations. In this case, the influence of the null traces (that were assigned to missing offset positions) was reduced by the inclusion of the data weighing matrix $W$.

## Summary

Least-squares AVA migration for common azimuth data has potential for deriving high resolution artifact-free CIG that can be subsequently used to extract rock properties and/or fluid indicators. It provides high quality common image gathers in angle domain and, in addition, a migrated image that can be used to reconstruct the seismic volume (de-migrate).

Our current implementation of LS migration uses the method of conjugate gradients in its simplest form. We are currently examining the possibility of using the total least-squares method (Arun, 1993) in an attempt to combat modeling operator errors and velocity mismatch as well as sampling related artifacts.

## Acknowledgments

The Signal Analysis and Imaging Group at the University of Alberta would like to acknowledge financial support from the following companies: Geo-X Ltd., Encana

Ltd., Veritas Geo-Services and the Schlumberger Foundation. This research has also been supported by The Natural Sciences and Engineering Research Council of Canada and the Alberta Department of Energy.

## References

Arun, K. S., 1993, A unitarily constrained total least squares problem in signal processing: SIAM J. Matris Anal. Appl. **13**, 729-745.

Biondi, B., and Palacharla, G., 1996, 3-D prestack migration of common-azimuth data: Geophysics, **61**, no.6, 1822-1832.

de Bruin, C. G. M., Wapenaar, C. P. A., and Berkhout, A. J., 1990, Angle-dependent reflectivity by means of prestack migration: Geophysics, **55**, no.9, 1223-1234.

Gazdag, J., and Sguazzero, P., 1984, Migration of seismic data by phase-shift plus interpolation: Geophysics, **49**, no.2, 124-131.

Hestenes, M., and Stiefel, E., 1952, Methods of conjugate gradients for solving linear systems: Nat. Bur. Standards J. Res., **49**, 403-436.

Kuehl, H. and Sacchi, M.D., 2001, Generalized least-squares DSR Migration using a common angle imaging condition: 71st Annual Mtg. SEG: Expanded Abstracts, 4 pages, CDROM.

Kuehl, H. and Sacchi, M.D., 2002, Robust AVP estimation using LS wave equation migration: 72nd Annual Mtg. SEG: Expanded Abstracts, 4 pages, CDROM.

Kuehl H. and Sacchi M.D., 2003, Least squares wave-equation migration for AVP/AVA inversion: Geophysics, **68**, no. 1, 262-273.

Mosher, C., and Foster, D., 2000, Common angle imaging conditions for prestack depth migration: 70th Ann. Interanat. Mtg., SEG Expanded Abstracts, 830-833.

Popovici, A. M., 1996, Prestack migration by split-step DSR: Geophysics, **61**, No.05, 1412-1416.

Prucha, M., Biondi, B., and Symes, W., 1999, Angle-domain common image gathers by wave-equation migration: 69th Ann. Interanat. Mtg., SEG Expanded Abstracts, 824-827.

Sava, P., Biondi, B., and Fomel, S., 2001 Amplitude-preserved common image gathers by wave-equation migration: 71st Ann. Interanat. Mtg., SEG Expanded Abstracts, 296-299.

Stolt, R. H., and Weglein, A. B., 1985, Migration and inversion of seismic data: Geophysics, **50**, no. 12, 2458-2472.

Xu, S., Chauris, H., Lambare, G., and Noble, M. S., 1998, Common angle image gather: A new strategy for imaging complex media: 68 th Ann. Interanat. Mtg., SEG Expanded Abstracts, 1538-1541.

Wapenaar, C. P. A., Van Wijingaarden, A. J., Van Geloven, W., and Van der Leij, T., 1999, Apparent AVA effects of fine layering: Geophysics, **64**, no. 6, 1939-1948.

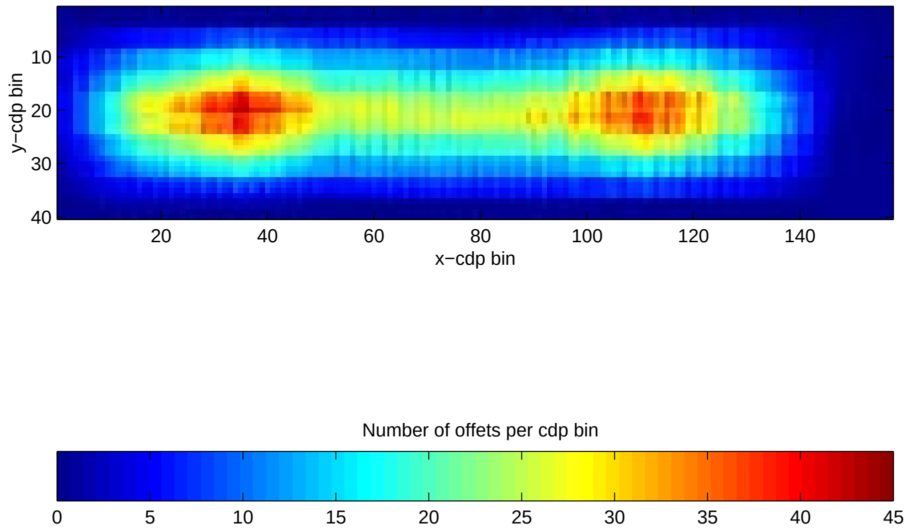


Fig. 1: Distribution of offset for the field data utilized to test our least-squares 3D wave equation AVA imaging algorithm.

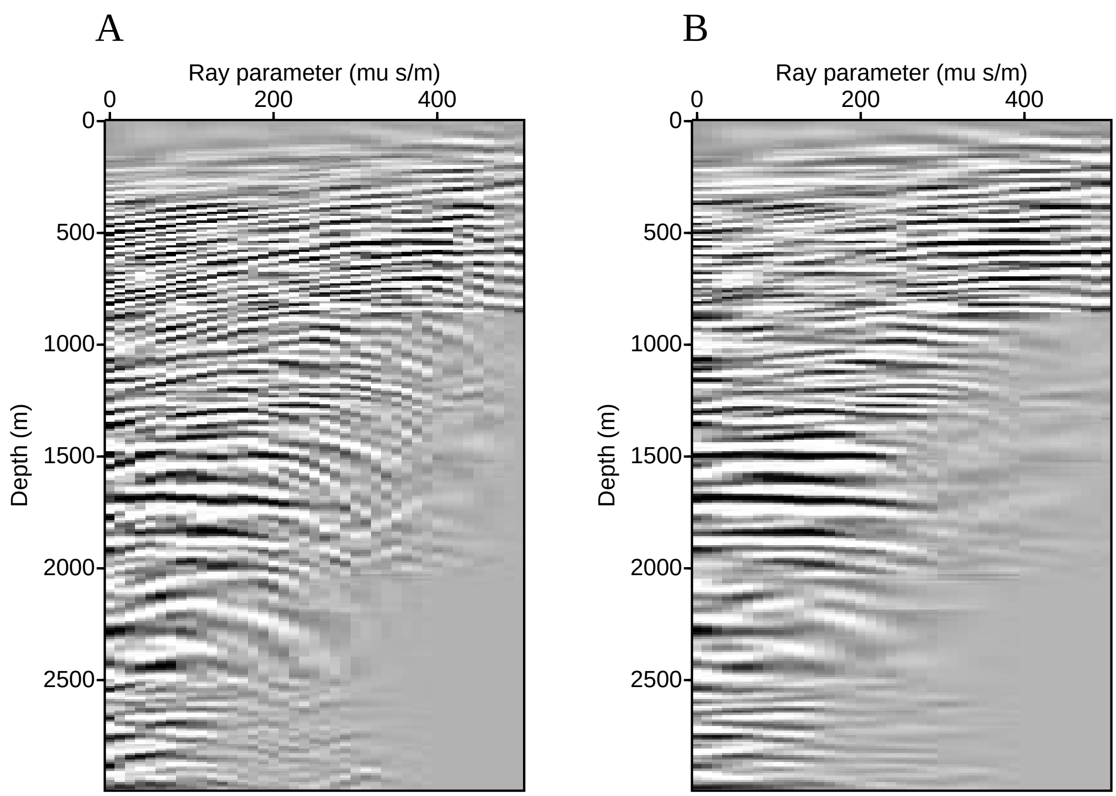


Fig. 2: (A) AVP gather obtained via direct migration of the pre-stack volume after binning. Null traces were assigned to missing offset positions. (B) AVP gather obtained via LS wave equation AVP migration after 4 conjugate gradients iterations.